Palestine Journal of Mathematics

Vol 14(1)(2025) , 164–182

A new variant of third order WENO scheme with increasingly higher order of accuracy for hyperbolic conservation laws

Anurag Kumar, Bhavneet Kaur and Neeraj Kumar Tripathi

Communicated by Ayman Badawi

MSC 2010 Classifications: Primary 70K70; Secondary 35L65.

Keywords and phrases: WENO, Hyperbolic Equations, Smoothness Indicator, Order of Accuracy.

The authors would like to thank the reviewers and editor for their constructive comments and valuable suggestions that improved the quality of our paper.

Abstract In this paper, we propose an enhanced version of a third order finite difference WENO-L3 scheme to improve order of accuracy and resolutions of one- and two- dimensional hyperbolic conservation laws. Similar to other third order WENO schemes, the improved WENO scheme uses three points stencil $\{x_{i-1}, x_i, x_{i+1}\}$. The reconstruction process of numerical flux approximation is the convex combination of a second degree polynomial and two linear polynomials. We add an extra weight to less smooth sub-stencils of the domain which plays an important role to improve high resolution of the solutions especially at sharp gradients or discontinuities. We have shown the behaviour of the proposed scheme for a collection of scalar, one-dimensional as well as two-dimensional test problems. Numerous computational solutions strongly support that the proposed third order WENO scheme provides less truncation errors in L_1 and L_∞ norms with better resolution near discontinuities than other WENO schemes.

1 Introduction

Hyperbolic conservation laws describe a wide collection of developments in different disciplines such as astrophysical modelling, gas dynamics, meteorology, weather prediction, aerodynamics, also, in mathematical physics like shock turbulence interaction, hypersonic flying objects, etc. In the last three decades, several methodologies on higher order shock capturing schemes are developed by research community to explore the approximated solutions at critical and non-critical points for hyperbolic conservation laws. The aim of the present article is to propose a new third order finite difference weighted essentially non-oscillatory (WENO) scheme. Initially, the first WENO scheme was developed by Liu, Osher and Chan [1] as an extension of essentially non-oscillatory (ENO) scheme to explore the approximate solutions for the hyperbolic conservation laws, given by

$$\begin{cases} u_t + \nabla . f(u) = 0, \\ u(x_1, x_2, ..., x_n, 0) = u_0(x_1, x_2, ..., x_n). \end{cases}$$

These type of non-linear complex systems do not have the analytical solutions, if they have, they contain strongly irregular solutions which also may obtain complicated smooth solution region structures. The existence of shocks, rarefaction waves and contact discontinuities in the solution profile make it difficult to be high order accurate and stable numerical schemes due to the growth of numerical instabilities and spurious oscillations.

Weighted essentially non-oscillatory (WENO) scheme is one of the most important shock capturing and high resolution scheme which is improved by various authors as central WENO [2] and compact WENO [3] and Hermite WENO [4] schemes to solve problems coming up in science and engineering in past two decades. Jiang and Shu [5] developed the WENO scheme with finite difference framework (WENO-JS) which contains a stencil with $(2r-1)$ points and r substencils with r points. A general framework for designing a new non-linear weighting

procedure is also presented in this paper that provides the final approximation to be of order $(2r-1)$. They developed a fifth order WENO-JS $(r = 3)$ scheme by using these formulations. Balsara and Shu [6] constructed a class of monotonicity preserved schemes which are a higher order extension of finite difference WENO-JS scheme up to eleventh order. Borges et al. [7] developed a new technique of weight formulation with high order smoothness indicators to improve the WENO-JS scheme which is marked as WENO-Z. They showed that the fifth order WENO-Z scheme achieves better accuracy and higher resolutions with lower dissipation than WENO-JS. The WENO-Z scheme also avoids the loss of accuracy near critical points similar as WENO-M but with better computational efficiency. Yamaleev et al. [8] presented a third order energy stable finite difference WENO (ESWENO) scheme to improve the approximate solutions of piecewise continuous initial problems for hyperbolic conservation laws. However, the ESWENO scheme works for limited applications. Castro et al. [9] constructed a generalized approach for global smoothness indicator to improve the desired order of accuracy of all odd order WENO-Z schemes. The accuracy analysis of a finite difference WENO scheme has been carried out by Borges et al. in [10] to derive the alternative proof of the sufficient condition. A hybrid WENO scheme [11] is introduced by applying a novel switch of third order WENO and fourth order central WENO schemes, recognized as WENO-N3. An improved third order WENO scheme by presenting a new global smoothness indicator is pronounced as WENO-NP3 [12, 13, 14]. Various third order WENO schemes were also further improved and reported in [15, 16, 17, 18] as well as by Xu and Wu in [19, 20]. A third order WENO-AB3 scheme with modified global smoothness indicator is constructed to improve order of accuracy at critical points by Anurag and Bhavneet in [21]. They have also introduced a modified fifth order WENO-NZ5 scheme in [22]. Zhu et.al have proposed a fifth order finite difference WENO (WENO-ZQ5) scheme [23] by defining a different polynomial reconstruction procedure which is written in the convex combination of a second degree polynomial with two linear polynomials in traditional WENO fashion. The related optimal weights are set to be any random positive numbers with their sum equals one. Later, they have introduced the same criteria for finite volume framework [24] also. Guodong Li et al. [25] presented an improved third order finite difference WENO scheme for the optimal stencil for hyperbolic conservation laws which is an extension of WENO-ZQ5 scheme. The authors also made a small difference from WENO-ZQ scheme on the global smoothness indicator. Xu and Wu have presented the WENO-P3 scheme [20] by adding new term in the non-linear weights of the WENO-N3 scheme. Several authors have presented important concepts in [26, 27, 28, 29, 30, 31, 32, 33, 34] to understand the methods. Based on above status of research, we present an improved version of third order WENO-L3 scheme to achieve desired convergence order. A new polynomial reconstruction procedure is defined by using the information of a three-points stencil and two smaller two-points substencils. The non-linear weighting procedure is also formulated by using a new global smoothness indicator in the form of linear combination of first derivative of the smoothness indicator of the stencil $S_0\{x_{i-1}, x_i, x_{i+1}\}$ and two lower order smoothness indicators for $S_1\{x_{i-1}, x_i\}, S_2\{x_i, x_{i+1}\}$. For convenience, we denote as the proposed scheme as WENO-L3+ scheme.

The article proceeds as follows: In section 2, we deal with usual preliminaries of basic formulation of conventional third order finite difference WENO schemes. In section 3, we introduce the new finite difference WENO scheme in third order manner and analyze its basic properties by using the Taylor series expansion in detail. In section 4, the computational results of the proposed scheme are compared with other variants of third order WENO scheme for a number of benchmark smooth initial test cases or test cases where the solution has shocks and discontinuities. In the end, the conclusion and related discussion are presented in the section 5.

2 Finite difference WENO schemes

For simplicity, we describe the brief formulation of the conservative finite difference weighted essentially non-oscillatory (WENO) scheme. We apply it to one-dimensional hyperbolic equations in conservative form with the initial condition

$$\frac{\partial u}{\partial t} + \frac{\partial f(u)}{\partial x} = 0, \tag{2.1}$$
$$u(x, 0) = u_0(x).$$

The solution $u(x,t)$ is a function of x as spatial variable and t as time variable. The flux function $f(u)$ is divided into two parts as $f(u) = f^+(u) + f^-(u)$ to preserve the numerical stability and avoid entropy violating solution where both functions $f^+(u)$ and $f^-(u)$ satisfy the derivative conditions $\frac{df^+(u)}{du} \geq 0$ and $\frac{df^-(u)}{du} \leq 0$, respectively. We distribute the uniform mesh into the cells $[x_{i-1/2}, x_{i+1/2}]$ with the cell sizes $h = x_{i+1/2} - x_{i-1/2}$ and the cell centers as $x_i = \frac{1}{2}(x_{i+1/2} + x_{i-1/2})$. Several flux splitting methods are used in the research papers but the global Lax-Friedrichs splitting criterion is heavily applied because of its capability to produce smooth fluxes. According to this criterion, the functions $f^+(u)$, $f^-(u)$ are written as $f^+(u) = \frac{1}{2}(f(u) + \lambda u)$ and $f^-(u) = \frac{1}{2}(f(u) - \lambda u)$, respectively. The constant $\lambda = \max_u(|f'(u)|)$ comes out from the whole applicable range of u. We determine the semi-discrete form [5] by integrating eqn. (2.1) with respect to x while keeping the time variable continuous.

$$\frac{du_i}{dt} = -\frac{1}{h}\left(\overline{f}_{i+1/2} - \overline{f}_{i-1/2}\right) = L(u_i). \tag{2.2}$$

The eqn. (2.2) is a system of time dependent ordinary differential equations (ODEs) which holds the spatial accuracy of the scheme. The reconstruction procedure is defined only for the positive flux function $\overline{f}^+_{i+1/2}$. For convenience, we drop the superscript '+'. Similarily, we can evaluate the negative numerical flux function $\overline{f}^-_{i+1/2}$ about $x_{i+1/2}$ by using mirror symmetric rule then a numerical flux approximation is set to be $\overline{f}_{i+1/2} = \overline{f}^+_{i+1/2} + \overline{f}^-_{i+1/2}$.

2.1 WENO-JS3 scheme [5]

A third order WENO reconstruction process uses a three-point stencil $S_0\{x_{i-1}, x_i, x_{i+1}\}$ which is split into two- point substencils $S_1\{x_{i-1}, x_i\}, S_2\{x_i, x_{i+1}\}$. The numerical flux approximation at $x_{i+\frac{1}{2}}$ is defined as the convex combination of the interpolated values for both substencils. The interpolated values $f_{1,i+1/2}$, $f_{2,i+1/2}$ for S_1 and S_2 are given, respectively as:

$$f_{1,i+1/2} = -\frac{1}{2}f_{i-1} + \frac{3}{2}f_i,$$
$$f_{2,i+1/2} = \frac{1}{2}f_{i+1} + \frac{1}{2}f_i.$$

The resultant approximation flux at $x_{i+\frac{1}{2}}$ for third order WENO scheme is

$$\overline{f}_{i+1/2} = w_1 f_{1,i+1/2} + w_2 f_{2,i+1/2},$$

where w_1 and w_2 are the non-linear weight functions suggested by Jiang and Shu. The authors provide the classical weighting procedure as follows:

$$\begin{cases} w_k = \frac{\alpha_k}{\alpha_1+\alpha_2}, \\ \alpha_k = \frac{d_k}{(\beta_k+\varepsilon)^2}, \ k = 1, 2. \end{cases} \tag{2.3}$$

The constants $d_1 = \frac{1}{3}$, $d_2 = \frac{2}{3}$ are the optimal weights and a small positive number $\varepsilon = 10^{-6}$ is used to avoid the division to be zero in the denominator. The general smoothness indicator formula for an interpolated polynomial with respect to a stencil can be written as:

$$\beta_k = h\int_{x_{i-\frac{1}{2}}}^{x_{i+\frac{1}{2}}} \left(\frac{d\overline{f}_k}{dx}\right)^2 dx + h^3 \int_{x_{i-\frac{1}{2}}}^{x_{i+\frac{1}{2}}} \left(\frac{d^2\overline{f}_k}{dx^2}\right)^2 dx. \tag{2.4}$$

$$\beta_k = \dot{\beta}_k + \ddot{\beta}_k \tag{2.5}$$

where $\dot{\beta}_k$, $\ddot{\beta}_k$ are the first and second integrals of the smoothness indicator formula given in eqn. (2.4). The β_1 and β_2 are the smoothness indicators for both substencils which are expressed to determine the numerical flux approximation $f_{k,i+1/2}$.

$$\beta_1 = (f_i - f_{i-1})^2,$$
$$\beta_2 = (f_{i+1} - f_i)^2. \tag{2.6}$$

The weighting procedure expressed in eqn. (2.3) fails to achieve the desired convergence rate.

2.2 WENO-Z3 scheme

Borges et al. [7] presented a non-linear weighting procedure by using a global smoothness indicator τ_Z containing whole three-point stencil $S_0\{x_{i-1}, x_i, x_{i+1}\}$ which obtains higher order accuracy than the classical smoothness indicator. An analysis of the convergence rate has been done by the authors to solve the issue for vanishing the lower order derivatives at critical points. A global smoothness indicator τ_Z for third order WENO scheme is given by

$$\tau_Z = |\beta_1 - \beta_2|.$$

The non-linear weight functions by using τ_Z are presented as:

$$\begin{cases} w_k = \frac{\alpha_k}{\alpha_1+\alpha_2}, \\ \alpha_k = d_k\Big(1 + \frac{\tau_Z}{\beta_k+\varepsilon}\Big), \ k = 1, 2. \end{cases}$$

with $\varepsilon = 10^{-40}$.

2.3 WENO-L3 Scheme

The interpolated polynomial for whole stencil $S_0\{x_{i-1}, x_i, x_{i+1}\}$ is given by

$$f_{0,i+1/2} = \frac{1}{6}(-f_{i-1} + 5f_i + 2f_{i+1}). \tag{2.7}$$

The authors obtain the local smoothness indicator for the reconstructed polynomial (2.7) which is written as

$$\beta_0 = \frac{13}{12}(f_{i-1} - 2f_i + f_{i+1})^2 + \frac{1}{4}(f_{i+1} - f_{i-1})^2. \tag{2.8}$$

$$w_k = \frac{\alpha_k}{\alpha_0 + \alpha_1 + \alpha_2}, \ \ k = 0, 1, 2 \tag{2.9}$$

where

$$\alpha_k = d_k\Big(1 + \frac{\tau}{\beta_k + \varepsilon}\Big), \tag{2.10}$$

and

$$\tau = \left(\frac{(\beta_0 - \beta_1) + (\beta_0 - \beta_2)}{2}\right)^2, \ \ \varepsilon = 10^{-40}. \tag{2.11}$$

The final reconstruction of the numerical flux approximation at $x = x_{i+\frac{1}{2}}$ is written as:

$$\overline{f}_{i+1/2} = w_0 f_{0,i+1/2} + w_1 f_{1,i+1/2} + w_2\Big(\frac{1}{d_2} f_{2,i+1/2} - \frac{d_0}{d_2} f_{0,i+1/2} - \frac{d_1}{d_2} f_{1,i+1/2}\Big).$$

Guodong Li et al. [25] have performed all numerical results of WENO-L3 with different type of linear weights same as WENO-ZQ5 [23] scheme which are (1) $d_0 = 0.98$, $d_1 = 0.01$ and $d_2 = 0.01$ (2) $d_0 = \frac{1}{3}$, $d_1 = \frac{1}{3}$ and $d_2 = \frac{1}{3}$ (3) $d_0 = 0.01$, $d_1 = 0.495$ and $d_2 = 0.495$. The authors have shown that the WENO-L3 scheme achieves desired rate of convergence where first and second derivatives vanish but the third derivative is nonzero.

Sufficient condition

A sufficient condition to develop a new third order accurate WENO scheme is obtained in [35] by Henrick et al., also in [8] by Yamaleev et al.. The condition for an overall third order accurate WENO scheme is given as:

$$w_k^{\pm} - d_k = O(h^2), \ k = 0, 1 \tag{2.12}$$

where the non-linear weights w_k^+ and w_k^- are used to make the combinations of $f_{k,i+1/2}$ and $f_{k,i-1/2}$, respectively.

3 Improved scheme

With the choice of one entire stencil $S_0\{x_{i-1}, x_i, x_{i+1}\}$ and two sub-stencils $S_1\{x_{i-1}, x_i\}, S_2\{x_i, x_{i+1}\}$ already chosen, we write the smoothness indicator β_0 for S_0 by using the smoothness indicator formula (2.4) as

$$\beta_0 = \frac{13}{12}\left(f_{i-1} - 2f_i + f_{i+1}\right)^2 + \frac{1}{4}\left(f_{i-1} - f_{i+1}\right)^2. \tag{3.1}$$

We write β_0 as the sum of $\dot{\beta}_0$ and $\ddot{\beta}_0$

$$\beta_0 = \dot{\beta}_0 + \ddot{\beta}_0\ . \tag{3.2}$$

Hence, eqn. (3.1) can be written as

$$\beta_0 = \frac{1}{12}\left(f_{i-1} - 2f_i + f_{i+1}\right)^2 + \frac{1}{4}\left(f_{i-1} - f_{i+1}\right)^2 + \left(f_{i-1} - 2f_i + f_{i+1}\right)^2. \tag{3.3}$$

By comparing eqns. (3.2) and (3.3), the first and second derivatives of β_0 are as follows

$$\begin{cases} \dot{\beta}_0 = \frac{1}{12}\left(f_{i-1} - 2f_i + f_{i+1}\right)^2 + \frac{1}{4}\left(f_{i-1} - f_{i+1}\right)^2, \\ \ddot{\beta}_0 = \left(f_{i-1} - 2f_i + f_{i+1}\right)^2. \end{cases} \tag{3.4}$$

We write the Taylor series expansions at x_i of the local smoothness indicators given in eqn. (2.6) and $\dot{\beta}_0$ from eqn. (3.4) as

$$\begin{aligned} \beta_1 = {} & f_i'^2h^2 - f'f_i''h^3 + \left(\frac{1}{4}f_i''^2 + \frac{1}{3}f_i'f_i'''\right)h^4 - \frac{1}{12}f_i'f_i^{(4)}h^5 - \frac{1}{6}f_i''f_i'''h^5 + \left(\frac{1}{60}f_i'f_i^{(5)} + \frac{1}{24}f_i''f_i^{(4)} + \right. \\ & \left. \frac{1}{36}f_i'''^2\right)h^6 - \frac{1}{360}f_i'f_i^{(6)}h^7 - \frac{1}{120}f_i''f_i^{(5)}h^7 - \frac{1}{72}f_i'''f_i^{(4)}h^7 + \frac{1}{2520}f_i'f_i^{(7)}h^8 + \frac{1}{720}f_i''f_i^{(6)}h^8 + \\ & \frac{1}{360}f_i'''f_i^{(5)}h^8 + \frac{1}{576}f_i'(f_i^{(4)})^2h^8 + O(h^9). \end{aligned} \tag{3.5}$$

$$\begin{aligned} \beta_2 = {} & f_i'^2h^2 + f'f_i''h^3 + \left(\frac{1}{4}f_i''^2 + \frac{1}{3}f_i'f_i'''\right)h^4 + \frac{1}{12}f_i'f_i^{(4)}h^5 + \frac{1}{6}f_i''f_i'''h^5 + \left(\frac{1}{60}f_i'f_i^{(5)} + \frac{1}{24}f_i''f_i^{(4)} + \right. \\ & \left. \frac{1}{36}f_i'''^2\right)h^6 + \frac{1}{360}f_i'f_i^{(6)}h^7 + \frac{1}{120}f_i''f_i^{(5)}h^7 + \frac{1}{72}f_i'''f_i^{(4)}h^7 + \frac{1}{2520}f_i'f_i^{(7)}h^8 + \frac{1}{720}f_i''f_i^{(6)}h^8 + \\ & \frac{1}{360}f_i'''f_i^{(5)}h^8 + \frac{1}{576}f_i'(f_i^{(4)})^2h^8 + O(h^9). \end{aligned} \tag{3.6}$$

$$\dot{\beta}_0 = f_i'^2h^2 + \left(\frac{1}{12}f_i''^2 + \frac{1}{3}f_i'f_i'''\right)h^4 + \left(\frac{1}{60}f_i'f_i^{(5)} + \frac{1}{72}f_i''f_i^{(4)} + \frac{1}{36}f_i'''^2\right)h^6 + O(h^8).$$

We rewrite β_1, β_2 and $\dot{\beta}_0$ as

$$\begin{cases} \beta_1 = D(1 + O(h)), \\ \beta_2 = D(1 + O(h)), \\ \dot{\beta}_0 = D(1 + O(h^2)), \end{cases}$$

where $D = h^2(f_i')^2$ is a non-zero constant.
The two difference expansions $\dot{\beta}_0 - \beta_1$ and $\dot{\beta}_0 - \beta_2$ in Taylor series about f_i' can be written as:

$$\begin{aligned} \dot{\beta}_0 - \beta_1 = {} & f'f_i''h^3 - \frac{1}{6}f_i''^2h^4 + \left(\frac{1}{12}f_i'f_i^{(4)} + \frac{1}{6}f_i''f_i'''\right)h^5 - \frac{1}{36}f_i''f^{(4)}h^6 + \left(\frac{1}{360}f_i'f_i^{(6)} + \frac{1}{120}f_i''f_i^{(5)} + \right. \\ & \left. \frac{1}{72}f_i'''f_i^{(4)}\right)h^7 + O(h^8). \end{aligned} \tag{3.7}$$

$$\dot{\beta}_0 - \beta_2 = -f' f_i'' h^3 - \frac{1}{6} f_i''^2 h^4 - \Big(\frac{1}{12} f_i' f_i^{(4)} + \frac{1}{6} f_i'' f_i'''\Big) h^5 - \frac{1}{36} f_i'' f^{(4)} h^6 - \Big(\frac{1}{360} f_i' f_i^{(6)} + \frac{1}{120} f_i'' f_i^{(5)} + \frac{1}{72} f_i''' f_i^{(4)}\Big) h^7 + O(h^8). \tag{3.8}$$

The modified nonlinear un-normalized weights are expressed as

$$w_k = \frac{\alpha_k}{\sum_{s=0}^{2} \alpha_s}, \; k = 0, 1, 2 \tag{3.9}$$

where

$$\alpha_k = d_k \left(1 + \left(\frac{\tau_{L+} + \varepsilon}{\beta_k + \varepsilon}\right) + \zeta_k\right), \tag{3.10}$$

and 'ε' is a small positive number. The criteria to choose the value of ε is presented in subsection (3.2). The proposed WENO scheme is termed as " WENO-L3+ " scheme which is an improved varient of WENO-L3 scheme. The computational cost also can be minimized by using the weights in aforesaid form.

By using the procedure of Acker et al. [17] and Gande et al. [36], we have studied the nature and properties of ζ_k and is formulated as

$$\zeta_k = \lambda\Big(\frac{\beta_k + \varepsilon}{\tau_{L+} + \varepsilon}\Big). \tag{3.11}$$

The parameter λ controls the increase in the weight given to the less smooth substencils and maintains the non-oscillatory property of the scheme as well. The improved global smoothness indicator τ_{L+} is defined as

$$\tau_{L+} = \frac{\{(\dot{\beta}_0 - \beta_1) + (\dot{\beta}_0 - \beta_2)\}^2}{32}. \tag{3.12}$$

By adding eqns. (3.7) and (3.8), we obtain

$$(\dot{\beta}_0 - \beta_1) + (\dot{\beta}_0 - \beta_2) = -\frac{1}{3} f_i''^2 h^4 - \frac{1}{18} f_i'' f^{(4)} h^6 + O(h^8). \tag{3.13}$$

From eqns. (3.12) and (3.13), we derive

$$\tau_{L+} = \frac{\Big(-\frac{1}{3} f_i''^2 h^4 - \frac{1}{18} f_i'' f^{(4)} h^6 + O(h^8)\Big)^2}{32} = O(h^8). \tag{3.14}$$

The final reconstruction of the numerical flux approximation at $x = x_{i+\frac{1}{2}}$ is written as:

$$\overline{f}_{i+1/2} = w_0\Big(\frac{1}{d_0} f_{0,i+1/2} - \frac{d_1}{d_0} f_{1,i+1/2} - \frac{d_2}{d_0} f_{2,i+1/2}\Big) + w_1 f_{1,i+1/2} + w_2 f_{2,i+1/2}.$$

3.1 Convergence analysis of the proposed scheme

In this section, we satisfy the optimality condition (2.12) for the third order WENO scheme. The optimality condition requires that the value of the control parameter λ does not increase as h decreases. It should not be very insignificant too because the intention of adding an extra weight is to improve the resolution of the computational solutions. Hence, we choose $\lambda = O(h^t)$ where $0 < t < 1$, implying $\lambda = O(1)$.

The truncation error analysis of the non-linear weights (3.9) for the proposed scheme is given as follows:

$$\alpha_k = d_k \left(1 + \left(\frac{O(h^8) + \varepsilon}{O(h^2) + \varepsilon}\right) + h^t \left(\frac{O(h^2) + \varepsilon}{O(h^8) + \varepsilon}\right)\right). \tag{3.15}$$

We assume $\varepsilon = 0$ in the eqn. (3.15) as it does not effect the overall scheme but plays an important role in finding better resolution in the computational solutions. We thus obtain

$$\alpha_k = d_k \left(1 + \left(\frac{O(h^8)}{O(h^2)}\right) + h^t \left(\frac{O(h^2)}{O(h^8)}\right)\right) = d_k\Big(1 + O(h^{t-6})\Big), \tag{3.16}$$

where $0 < t < 6$. This is contradiction as $0 < t < 1$. Therefore, the convergence of the nonlinear weights w_k in eqn. (3.9) can not be assured to the optimal weights d_k as $h \to 0$. It may effect the computational results of the WENO-L3+ scheme to obtain higher resolution and order three. The ENO property [1] for continuous region $w_k = O(1)$ is also not satisfied because of negative powers of h in eqn. (3.16).

3.2 The role of ε in the proposed scheme

Now, we determine the nature of ε in terms of cell size h for the proposed scheme. We prefer $\varepsilon = O(h^q)$. It can be easily noted that $O(h^q) \to 0$ as $h \to 0$ only if $q > 0$. Therefore, we obtain the following inequality from eqn. (3.15).

$$\min\{\min\{8, q\} - \min\{2, q\}, t + \min\{2, q\} - \min\{8, q\}\} \geq 0. \tag{3.17}$$

The eqn. (3.17) implies

$$\begin{cases} \min\{8, q\} - \min\{2, q\} \geq 0, \\ t + \min\{2, q\} - \min\{8, q\} \geq 0. \end{cases} \tag{3.18}$$

We observe that the inequalities (3.18) are satisfied for $q \leq 2$. While choosing the value $\varepsilon \geq h^2$, it should be noticed that the larger value of ε may also obtain greater dissipation. We can write the above analysis as the proposition form.

Proposition 1: Suppose there are arbitrary number of vanishing derivatives in the problem and $\alpha_k = d_k(1 + O(h^m))$. Then the dominating term containing the cell size, i.e., $O(h^m)$ tends to 0 only when $\varepsilon \geq h^2$.[36]

3.3 Time discretization

For the time discretization, we use strong stability preserving (SSP) Runge-Kutta time-stepping [37] method of order three for all the test problems:

$$u^{(1)} = u^n + \Delta t L(u^n),$$

$$u^{(2)} = \frac{3}{4}u^n + \frac{1}{4}u^{(1)} + \frac{1}{4}\Delta t L(u^{(1)}),$$

$$u^{(n+1)} = \frac{1}{3}u^n + \frac{2}{3}u^{(2)} + \frac{2}{3}\Delta t L(u^{(2)}).$$

4 Computational results

In this section, a series of various computational results involving one- and two-dimensional initial test problems taken from many literatures are illustrated to assess the performance of new proposed scheme (WENO-L3+). We perform all numerical results of WENO-L3+ scheme by choosing linear weights as: $d_0 = 0.98$, $d_1 = 0.01$ and $d_2 = 0.01$. The values of ε and control parameter λ are set to be h^2 and $h^{\frac{1}{3}}$, respectively. We use the third-order TVD Runge–Kutta method with the time step $\Delta t \sim h^{\frac{3}{2}}$ to ensure Third-order convergence rate for accuracy test. The value of CFL=0.95 is chosen for all Lax and shock wave interaction test problems, also CFL=0.55 for all two dimensional test problems. We test the convergence order and accuracy of the WENO-JS3, WENO-Z3, WENO-L3 and WENO-L3+ schemes for linear as well as non-linear equations. The accuracy of the WENO schemes are obtained by using L_1 and L_∞ error norms which are defined for error 'e'over the domain $[c, d]$ as

$$\|e\|_\infty = \max_i |u_i - (u_h)_i|,$$

$$\|e\|_1 = \frac{d-c}{N+1} \sum_i |u_i - (u_h)_i|,$$

where N is the number of subdivisions of the domain and u_i and $(u_h)_i$ are the exact and approximate solutions ($h = \frac{d-c}{N}$) at the point x_i, respectively.

Linear advection equation

In order to verify the accuracy and rate of convergence, we discuss the linear advection equation with various initial test problems.

$$u_t + u_x = 0, \quad -1 \leq x \leq 1, \quad t > 0 \tag{4.1}$$

$$u(x, 0) = u_0(x).$$

4.1 Test problem: 1

We consider an smooth initial test problem

$$u_0(x) = \sin(\pi x). \tag{4.2}$$

Tables 1 and 2 present the comparison of L_1 and L_∞ errors and their orders between WENO-JS3, WENO-Z3, WENO-L3 and WENO-L3+ schemes. We can easily observe that the WENO-L3+ scheme attains third order of accuracy at critical points. The rate of convergence for WENO-JS3 scheme is greater than three at number of grid points 640 or more because the computational results are also dependent on the value of ε. The errors for WENO-L3+ scheme are smaller than WENO-JS3 and WENO-Z3 schemes. The magnitude of L_1 and L_∞ errors with their corresponding rate of convergence of WENO L3+ scheme are comparable with WENO-L3 scheme as the number of grid points increases.

N	WENO-JS3	WENO-Z3	WENO-L3	WENO-L3+
20	1.79747e-01(-)	1.42386e-01(-)	2.12105e-02(-)	2.02677e-02(-)
40	7.60505e-02(1.24)	4.05018e-02(1.81)	2.69084e-03(2.98)	2.57342e-03(2.98)
80	1.86722e-02(2.03)	9.57580e-03(2.08)	3.37381e-04(2.99)	3.22697e-04(2.99)
160	3.79179e-03(2.30)	2.10029e-03(2.19)	4.22018e-05(2.99)	4.03645e-05(2.99)
320	4.83703e-04(2.97)	4.46723e-04(2.23)	5.27625e-06(2.99)	5.04635e-06(3.00)
640	3.33412e-05(3.86)	9.41140e-05(2.25)	6.59554e-07(3.00)	6.30817e-07(3.00)
1280	1.93457e-06(4.11)	1.94948e-05(2.26)	8.24450e-08(3.00)	7.88528e-08(3.00)

Table 1: **A comparison study of L_1 errors and their orders of WENO schemes for eqn. (4.1) with eqn. (4.2) at the time till $t = 2.0$.**

N	WENO-JS3	WENO-Z3	WENO-L3	WENO-L3+
20	2.07938e-01(-)	1.49746e-01(-)	1.68512e-02(-)	1.60638e-02(-)
40	8.69414e-02(1.26)	5.87657e-02(1.35)	2.11516e-03(2.99)	2.04724e-03(2.97)
80	3.41233e-02(1.35)	2.21041e-02(1.41)	2.65011e-04(2.99)	2.55598e-04(3.00)
160	1.10823e-02(1.62)	8.11044e-03(1.44)	3.31461e-05(2.99)	3.18399e-05(3.00)
320	2.35907e-03(2.23)	2.92558e-03(1.47)	4.14399e-06(2.99)	3.98256e-06(3.00)
640	2.12643e-04(3.47)	1.04116e-03(1.49)	5.18014e-07(3.00)	4.95444e-07(3.00)
1280	7.98942e-06(4.73)	3.66408e-04(1.50)	6.47522e-08(3.00)	6.19310e-08(3.00)

Table 2: **A comparison study of L_∞ errors and their orders of WENO schemes for eqn. (4.1) with eqn. (4.2) at the time till $t = 2.0$.**

4.2 Test problem: 2

We opt another initial condition

$$u_0(x) = \sin^3(\pi x), \tag{4.3}$$

which contains first order critical points such that $u_x = 0$, $u_{xx} = 0$ and $u_{xxx} \neq 0$. The L_1, L_∞ errors and their corresponding rate of convergence for WENO-JS3, WENO-Z3, WENO-L3 and WENO-L3+ schemes are given in the tables 3 and 4 which show that the WENO-L3+ scheme achieves better errors and their corresponding orders than WENO-JS3 and WENO-Z3 schemes. We also observe from the figure (1) that WENO-L3+ provides equivalent results as WENO-L3 scheme. The rest of the discussion is same as test problem: 1.

N	WENO-JS3	WENO-Z3	WENO-L3	WENO-L3+
20	4.11849e-01(-)	3.73408e-01(-)	2.37566e-01(-)	2.29743e-01(-)
40	1.83414e-01(1.17)	1.14999e-01(1.70)	4.96542e-02(2.26)	4.76774e-02(2.27)
80	5.62879e-02(1.70)	2.98665e-02(1.94)	6.72928e-03(2.88)	6.44750e-03(2.89)
160	1.57866e-02(1.83)	6.72226e-03(1.49)	8.52962e-04(2.98)	8.16219e-04(2.98)
320	2.81026e-03(2.49)	1.42261e-03(2.24)	1.06828e-04(2.99)	1.02203e-04(3.00)
640	3.27085e-04(3.10)	2.94554e-04(2.27)	1.33595e-05(2.99)	1.27774e-05(3.00)
1280	2.31055e-05(3.82)	6.01963e-05(2.29)	1.67004e-06(3.00)	1.59728e-06(3.00)

Table 3: **A comparison study of L_1 errors and their orders of WENO schemes for eqn. (4.1) with eqn. (4.3) at the time till $t = 2.0$.**

N	WENO-JS3	WENO-Z3	WENO-L3	WENO-L3+
20	3.72710e-01(-)	3.24539e-01(-)	1.90565e-01(-)	1.86013e-01(-)
40	2.22210e-01 (0.75)	1.60482e-01(1.02)	4.03852e-02(2.24)	3.89236e-02(2.26)
80	9.47450e-02(1.23)	6.39015e-02(1.33)	5.48482e-03(2.88)	5.31596e-03(2.87)
160	3.71811e-02(1.35)	2.40272e-02(1.41)	6.94374e-04(2.98)	6.76573e-04(2.97)
320	1.15724e-02(1.68)	8.73997e-03(1.46)	8.69841e-05(2.99)	8.43167e-05(3.00)
640	2.29871e-03(2.33)	3.11926e-03(1.49)	1.08773e-05(2.99)	1.04052e-05(3.00)
1280	1.87727e-04(3.61)	1.09874e-03(1.51)	1.35977e-06(3.00)	1.30055e-06(3.00)

Table 4: **A comparison study of L_∞ errors and their orders of WENO schemes for eqn. (4.1) with eqn. (4.3) at the time till $t = 2.0$.**

4.3 Test problem 3

We consider an smooth initial test problem for critical points problems

$$u_0(x) = \sin\Big(\pi x - \frac{\sin(\pi x)}{\pi}\Big). \tag{4.4}$$

Tables 5 and 6 present the L_1, L_∞ errors and their corresponding rate of convergence for WENO-JS3, WENO-Z3, WENO-L3 and WENO-L3+ schemes. We notice from the numerical results that WENO-L3+ scheme achieves the desired order of accuracy. The magnitude of numerical errors of WENO-L3+ are obtained much better than WENO-JS3 and WENO-Z3 schemes but comparable with WENO-L3 scheme at each number of uniform grid points. The rest of the discussion is same as test problem: 1.

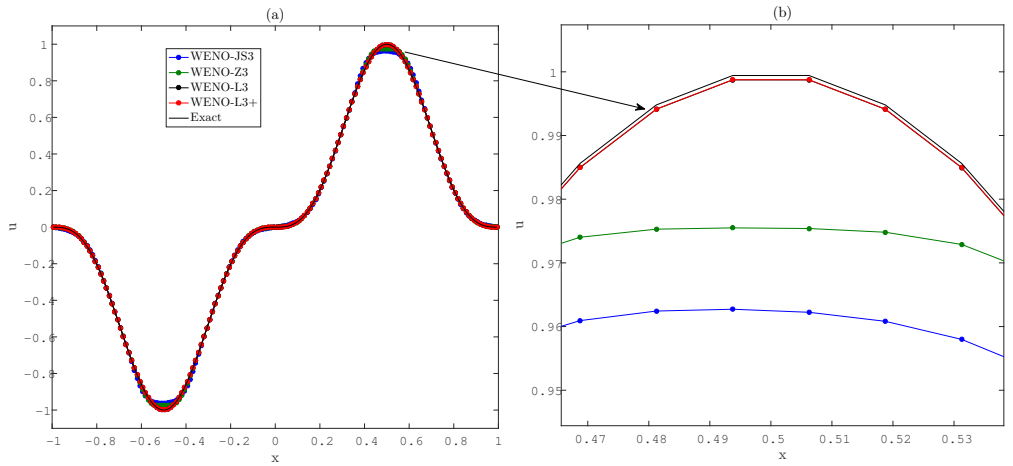

Figure 1: Numerical solutions (a) and enlarged portion (b) of eqn. (4.1) with eqn. (4.3) at the uniform grid points $N = 160$ and time $t = 2.0$.

N	WENO-JS3	WENO-Z3	WENO-L3	WENO-L3+
20	2.25871e-01(-)	1.52977e-01(-)	4.69852e-02(-)	4.51026e-02(-)
40	8.34609e-02(1.44)	4.73838e-02(1.69)	6.63191e-03(2.82)	6.34304e-03(2.83)
80	2.20960e-02(1.92)	1.13565e-02(2.06)	8.48426e-04(2.97)	8.11532e-04(2.97)
160	4.67512e-03(2.24)	2.53201e-03(2.17)	1.06499e-04(2.99)	1.01868e-04(2.99)
320	6.51804e-04(2.84)	5.44613e-04(2.22)	1.33237e-05(2.99)	1.27433e-05(3.00)
640	4.91290e-05(3.73)	1.13588e-04(2.26)	1.66568e-06(3.00)	1.59311e-06(3.00)
1280	2.90020e-06(4.08)	2.34699e-05(2.27)	2.08218e-07(3.00)	1.99146e-07(3.00)

Table 5: **A comparison study of L_1 errors and their orders of WENO schemes for eqn. (4.1) with eqn. (4.4) at the time till $t = 2.0$.**

N	WENO-JS3	WENO-Z3	WENO-L3	WENO-L3+
20	2.44722e-01 (-)	1.74287e-01(-)	5.32808e-02 (-)	5.12690e-02(-)
40	1.03930e-01(1.24)	6.97696e-02(1.32)	8.18187e-03(2.70)	7.81961e-03(2.71)
80	4.11544e-02(1.34)	2.66582e-02(1.39)	1.06377e-03(2.94)	1.01625e-03(2.94)
160	1.38541e-02(1.57)	9.85738e-03(1.43)	1.33976e-04(2.99)	1.28119e-04(2.99)
320	3.20311e-03(2.11)	3.55935e-03(1.47)	1.67650e-05(2.99)	1.60336e-05(3.00)
640	3.40994e-04(3.23)	1.25137e-03(1.50)	2.09603e-06(3.00)	2.00467e-06(3.00)
1280	1.43233e-05(4.57)	4.40886e-04(1.51)	2.62014e-07(3.00)	2.50613e-07(3.00)

Table 6: **A comparison study of L_∞ errors and their orders of WENO schemes for eqn. (4.1) with eqn. (4.4) at the time till $t = 2.0$.**

4.4 Burger's equation

We study the numerical results for the non-linear scalar Burger's equation:

$$u_t + \left(\frac{u^2}{2}\right)_x = 0, \ -1 \leq x \leq 1, \ \ t > 0 \tag{4.5}$$

along with the initial condition

$$u(x,0) = \frac{3}{10} + \frac{7}{10}\sin(\pi x). \tag{4.6}$$

The exact solution for eqn. (4.6) is smooth with time up to $t = 0.6363$, after this time it produces a moving shock which moves with a rarefaction wave. In order to verify the order of accuracy, we compute the solution when it is continuous. We take the final computational time $t = \frac{1}{\pi}$ for all the WENO schemes. Tables 7 and 8 present the L_1 and L_∞ errors for WENO-JS3, WENO-Z3, WENO-L3 and WENO-L3+ schemes along with their convergence rate. The magnitude of the errors of WENO-L3+ and WENO-L3 schemes are comparable in both norms but smaller than WENO-JS3 and WENO-Z3 schemes. We can easily observe from the tables that both WENO-L3+ and WENO-L3 schemes converge to the solution with convergence order of three for each number of grid points but are better than WENO-JS3 and WENO-Z3 schemes.

N	WENO-JS3	WENO-Z3	WENO-L3	WENO-L3+
20	3.44081e-02(-)	2.65937e-02(-)	1.74451e-02(-)	1.75132e-02(-)
40	8.79416e-03(1.97)	6.18841e-03(2.10)	3.04977e-03(2.51)	3.04605e-03(2.52)
80	2.34149e-03(1.91)	1.72589e-03(1.84)	4.24281e-04(2.84)	4.25338e-04(2.84)
160	4.81458e-04(2.28)	3.70445e-04(2.22)	5.25857e-05(3.01)	5.27335e-05(3.01)
320	5.23394e-05(3.20)	7.90443e-05(2.23)	6.42646e-06(3.03)	6.44744e-06(3.03)
640	6.49785e-06(3.01)	1.67867e-05(2.24)	7.87868e-07(3.03)	7.90449e-07(3.03)
1280	1.34434e-06 (2.27)	3.56533e-06(2.24)	9.72743e-08(3.02)	9.76008e-08(3.02)

Table 7: **A comparison study of L_1 errors and their orders of WENO schemes for eqn. (4.5) with eqn. (4.6).**

N	WENO-JS3	WENO-Z3	WENO-L3	WENO-L3+
20	5.19033e-02(-)	4.05149e-02(-)	6.48653e-02(-)	6.49257e-02(-)
40	1.99475e-02(1.38)	1.49669e-02(1.44)	1.61400e-02(2.00)	1.62219e-02(2.00)
80	7.44081e-03(1.42)	5.46402e-03(1.45)	3.64398e-03(2.14)	3.62615e-03(2.16)
160	2.19468e-03(1.76)	2.12052e-03(1.37)	5.24850e-04(2.80)	5.25170e-04(2.79)
320	3.01743e-04(2.86)	7.61980e-04(1.48)	6.54603e-05(3.00)	6.56249e-05(3.00)
640	1.95281e-05(3.95)	2.82273e-04(1.43)	7.97059e-06(3.04)	7.97970e-06(3.04)
1280	5.09557e-06(1.94)	1.03137e-04(1.45)	9.79481e-07(3.02)	9.80704e-07(3.02)

Table 8: **A comparison study of L_∞ errors and their orders of WENO schemes for eqn. (4.5) with eqn. (4.6).**

One-dimensional Euler system of conservation laws

In this subsection, we consider the one-dimensional Euler system of conservation laws which is given by:

$$\rho_t + (\rho u)_x = 0,$$
$$(\rho u)_t + (\rho u^2 + p)_x = 0,$$
$$E_t + (u(E+p))_x = 0,$$

where E is the total energy which can be determined by the equation $p = (\gamma - 1)(E - \frac{1}{2}\rho u^2)$ with $\gamma = 1.4$. ρ is the density variable and p is the pressure variable. The component u is the velocity vector towards x co-ordinate direction.

4.5 Lax test problem

Consider the Lax's shock tube test problem [38] for which the Riemnnn initial data is given by

$$(\rho, p, u) = \begin{cases} (1, 1, 0), & 0 \le x < 0.5 \\ (0.125, 0.1, 0), & 0.5 \le x \le 1 \end{cases} \tag{4.7}$$

The density solution for eqn. (4.7) are computed with grid points $N = 200$ up to time $t =$

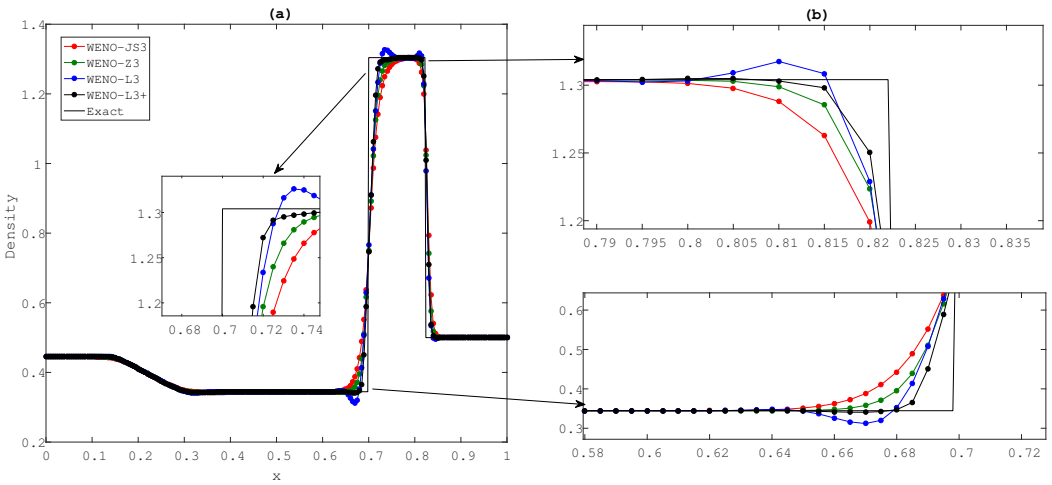

Figure 2: Density profile of Lax test problem (a) and enlarged portions (b) near the discontinuities.

0.13 along space direction. We study the density solutions obtained by WENO-JS3, WENO-Z3 and WENO-L3 schemes and compare them with WENO-L3+ scheme. The "exact"solution is computed at the grid points $N = 10,000$ with WENO-JS3 scheme. We can easily recognize from figure (2) that WENO-L3+ scheme provides better resolutions at the contact discontinuities and shocks accurately without overshoot and undershoot. The enlarged portions are given in figure (2b) in which we observe that the WENO-L3 scheme contains the overshoot and undershoot (see figure (7) in [25]). Finally, we observe that the performance of WENO-L3+ scheme is better than WENO-JS3, WENO-Z3 and WENO-L3 schemes.

4.6 Two blast wave interaction test problem

We consider one-dimensional two blast wave interaction test problem [39] which contains the initial data with reflective boundary conditions on both ends as follows:

$$(\rho, p, u) = \begin{cases} (1, 0, 1000), & 0 \le x < 0.1 \\ (1, 0, 0.01), & 0.1 \le x < 0.9 \\ (1, 0, 100), & 0.9 \le x \le 1 \end{cases} \tag{4.8}$$

The density solution with its enlarged portions near discontinuities for eqn. (4.8) are displayed in figures (3a), (3b) on the uniform grid points of $N = 800$, respectively. The CFL value for this test problem is taken as 0.95 and time up to $t = 0.038$. The "exact" solution is shown with WENO-JS3 scheme at the grid points $N = 10,000$. It can be clearly examined from the enlarged portions that all the WENO schemes provide accurate results at the extreme as well as discontinuities. Therefore, we conclude that WENO-L3+ scheme provides better resolution and converges to the exact solution better than WENO-JS3, WENO-Z3, WENO-L3 schemes.

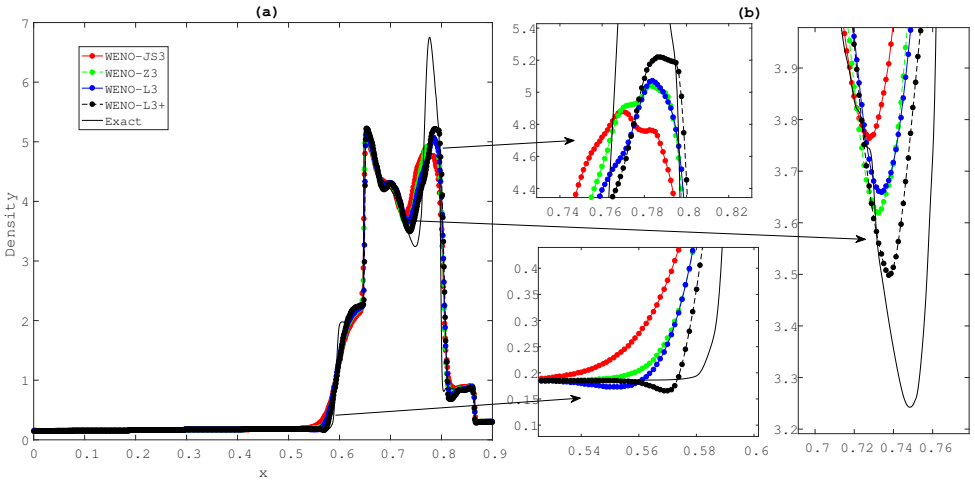

Figure 3: Density profile of two blast wave interaction test problem (a) and enlarged portions (b) near the discontinuities.

Two-dimensional Euler system of conservation laws

In this subsection, we consider the two-dimensional Euler system of conservation laws which is given by:

$$U_t + F(U)_x + G(U)_y = 0, \tag{4.9}$$

with $F(U) = (\rho u, p+\rho u^2, \rho uv, u(E+p))^T$, $U = (\rho, \rho u, \rho v, E)^T$, $G(U) = (\rho v, p+\rho v^2, \rho uv, v(E+p))^T$,
where E is the total energy determined by the equation $p = (\gamma - 1)(E - \frac{1}{2}\rho(u^2 + v^2))$ with $\gamma = 1.4$. ρ is the density variable, p is the pressure variable. The components u, v are the velocity vectors towards x and y co-ordinate directions. We demonstrate the computational results of various two-dimensional test problems for WENO-L3+ scheme and compare the results with WENO-JS3, WENO-Z3 and WENO-L3 schemes.

4.7 Configuration 3

We analyze the system of two-dimensional Euler equations with configuration 3 provided in detail by Lax and Liu [40]. We choose the square computational domain as $[0, 1] \times [0, 1]$. The initial constant values into four quadrants are divided by the lines $x = 0.8$ and $y = 0.8$ as follows:

$$(\rho, p, u, v) = \begin{cases} (1.5, 1.5, 0, 0), & 0.8 \le x \le 1,\ 0.8 \le y \le 1 \\ (0.5323, 0.30, 1.206, 0), & 0 \le x < 0.8,\ 0.8 \le y \le 1 \\ (0.138, 0.029, 1.206, 1.206), & 0 \le x < 0.8,\ 0 \le y < 0.8 \\ (0.5323, 0.30, 0, 1.206), & 0.8 < x \le 1,\ 0 \le y < 0.8 \end{cases}$$

The density profiles for WENO-JS3, WENO-Z3, WENO-L3 and WENO-L3+ schemes are computed in figure 4 with uniform grid points of 800×800. The computational time is taken upto

$t = 0.8$. According to a careful study of these results, it can be observed that the WENO-L3+ scheme provides better improvement in the resolution of portion of discrete vortices through the slip line roll-up than WENO-JS3, WENO-Z3 and WENO-L3 schemes.

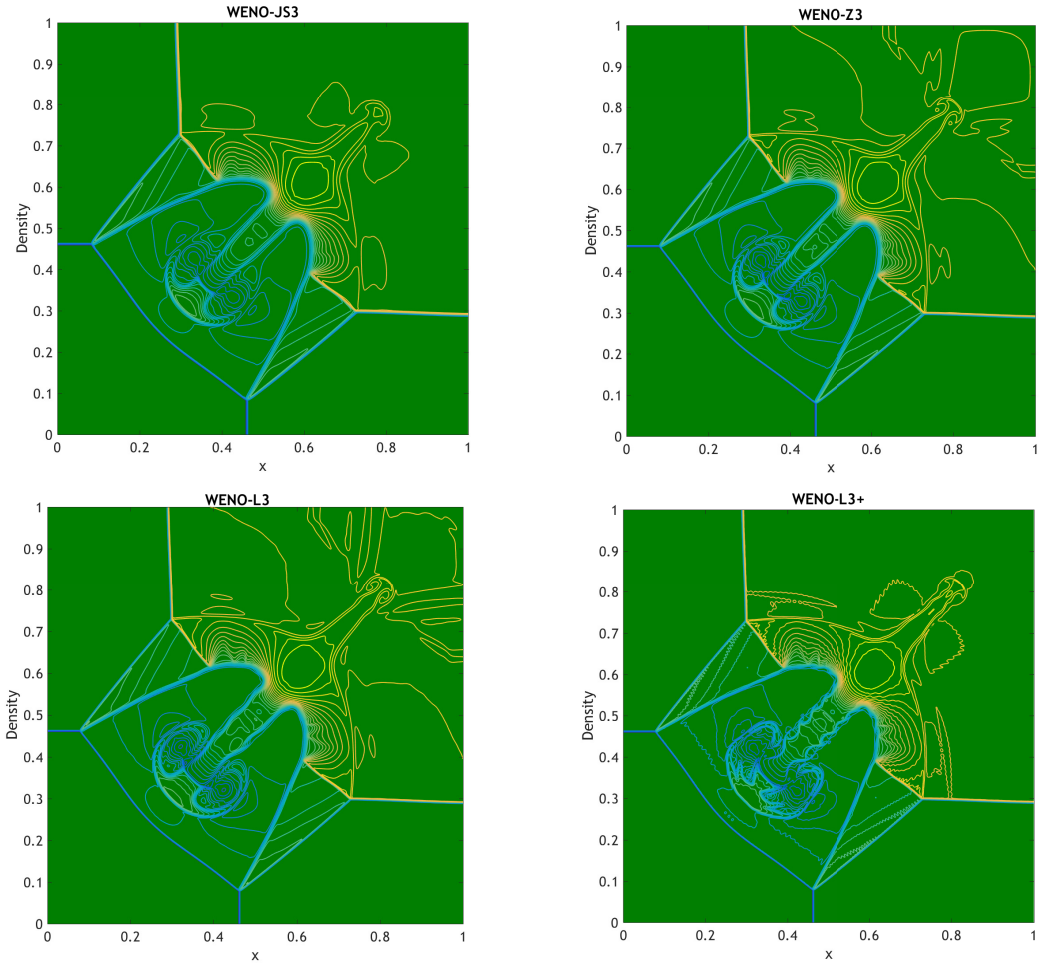

Figure 4: Density solutions for configuration 3 of WENO-JS3, WENO-Z3, WENO-L3 and WENO-L3+ schemes

4.8 Double Mach reflection (DMR) problem of a strong shock

The double Mach reflection problem, firstly introduced by Woodward and Colella (1984) is an important and standard test case which is widely used to check the ability of shock capturing and small scaled structure resolutions in two dimensional cases. According to the test problem, A right moving Mach 10 shock is placed at the beginning point $x = \frac{1}{6}$, $y = 0$ on the wall and the intersection angle between the shock and x-axis is 60°. The exact postshock condition is inflicted for the bottom boundary in the domain from $x = 0$ to $x = \frac{1}{6}$ and the reflective boundary condition is started from the point $x = \frac{1}{6}$ to $x = 4$. In the present simulation, the specific heat ratio γ is chosen as 1.4. The computational experiments are executed on the domain 4 units long and 1 unit high with fine grid points 1920×480 at the final time up to $t = 0.2$ and the CFL number 0.55. The initial data for the double Mach reflection problem is given by

$$(\rho, p, u, v) = \begin{cases} (8.0, 116.5, 7.145, -4.125), & x < \frac{1}{6} + \frac{y}{\sqrt{3}} \\ (1.4, 1.0, 0, 0), & x \geq \frac{1}{6} + \frac{y}{\sqrt{3}} \end{cases}$$

We present the numerical results in figure (5) for density contours obtained with WENO-JS3, WENO-Z3, WENO-L3 and WENO-L3+ schemes on the computational region $[0, 3] \times [0, 1]$.

Each of the schemes captures the shock waves really well. We also display partially close-up regions around the double Mach stems in figure (6) for all considered schemes. We can easily observe that the resolutions at the point of contact discontinuity for WENO-L3+ scheme are captured more clearly and yield improvement in the vortical structures. The resolving power of WENO-L3+ scheme is better than WENO-JS3, WENO-Z3 and WENO-L3 schemes.

5 Conclusion

In this article, a new method of third order finite difference WENO scheme for solving hyperbolic conservation laws, termed as WENO-L3+ is proposed. We have demonstrated a significant improvement in the computational results for third order WENO-L3+ scheme. In the proposed WENO scheme (WENO-L3+), a new polynomial reconstruction procedure is defined by using the information of a three-points and two smaller two-points spatial substencils. The non-linear weighting procedure is also formulated by using a new global smoothness indicator in the form of linear combination of first derivative of the smoothness indicator of the stencil $S_0\{x_{i-1}, x_i, x_{i+1}\}$ and two lower order smoothness indicators for $S_1\{x_{i-1}, x_i\}, S_2\{x_i, x_{i+1}\}$. We have shown the convergence analysis of the WENO-L3+ scheme by using Taylor series expansions and determined the desirable values of control parameter 'λ'and 'ε'. The computational experiments for several appropriate test problems are carried out to show the improvement of the WENO-L3+ scheme. The results obtained for several critical points problems have shown that the WENO-L3+ scheme achieves third order accuracy. It provides better performance than WENO-JS3 and WENO-Z3 schemes but comparable with WENO-L3 scheme. It can also be observed that WENO-L3+ scheme provided better resolution of solutions across shocks and discontinuities without producing spurious numerical oscillations than WENO-JS3, WENO-Z3 and WENO-L3 schemes. As a future topic of interest, the presented method can also be extended of the converegence order more than three.

References

[1] X.-D. Liu, S. Osher, T. Chan, *Weighted essentially non-oscillatory schemes*, Journal of computational physics **115** (1) (1994) 200–212.

[2] D. Levy, G. Puppo, G. Russo, *Central WENO schemes for hyperbolic systems of conservation laws*, ESAIM: Mathematical Modelling and Numerical Analysis **33** (3) (1999) 547–571.

[3] D. Ghosh, J. D. Baeder, *Compact reconstruction schemes with weighted ENO limiting for hyperbolic conservation laws*, SIAM Journal on Scientific Computing **34** (3) (2012) A1678–A1706.

[4] Y. H. Zahran, A. H. Abdalla, *Seventh order Hermite WENO scheme for hyperbolic conservation laws*, Computers & Fluids **131** (2016) 66–80.

[5] G.-S. Jiang, C.-W. Shu, *Efficient implementation of weighted ENO schemes*, Journal of computational physics **126** (1) (1996) 202–228.

[6] D. S. Balsara, C.-W. Shu, *Monotonicity preserving weighted essentially non-oscillatory schemes with increasingly high order of accuracy*, Journal of Computational Physics **160** (2) (2000) 405–452.

[7] R. Borges, M. Carmona, B. Costa, W. S. Don, *An improved weighted essentially non-oscillatory scheme for hyperbolic conservation laws*, Journal of Computational Physics **227** (6) (2008) 3191–3211.

[8] N. K. Yamaleev, M. H. Carpenter, *Third-order energy stable WENO scheme*, Journal of Computational Physics **228** (8) (2009) 3025–3047.

[9] M. Castro, B. Costa, W. S. Don, *High order weighted essentially non-oscillatory WENO-Z schemes for hyperbolic conservation laws*, Journal of Computational Physics **230** (5) (2011) 1766–1792.

[10] W.-S. Don, R. Borges, *Accuracy of the weighted essentially non-oscillatory conservative finite difference schemes*, Journal of Computational Physics **250** (2013) 347–372.

[11] X.-S. W. Y.-X. Zhao, *A high-resolution hybrid scheme for hyperbolic conservation laws*, International Journal for Numerical Methods in Fluids **78** (3) (2015) 162–187.

[12] X. Wu, J. Liang, Y. Zhao, *A new smoothness indicator for third-order WENO scheme*, International Journal for Numerical Methods in Fluids **81** (7) (2016) 451–459.

[13] S. Liu, Y. Shen, *Discontinuity-detecting method for a four-point stencil and its application to develop a third-order hybrid-WENO scheme*, Journal of Scientific Computing **81** (3) (2019) 1732–1766.

[14] S. Liu, Y. Shen, B. Chen, F. Zeng, *Novel local smoothness indicators for improving the third-order WENO scheme*, International Journal for Numerical Methods in Fluids **87** (2) (2018) 51–69.

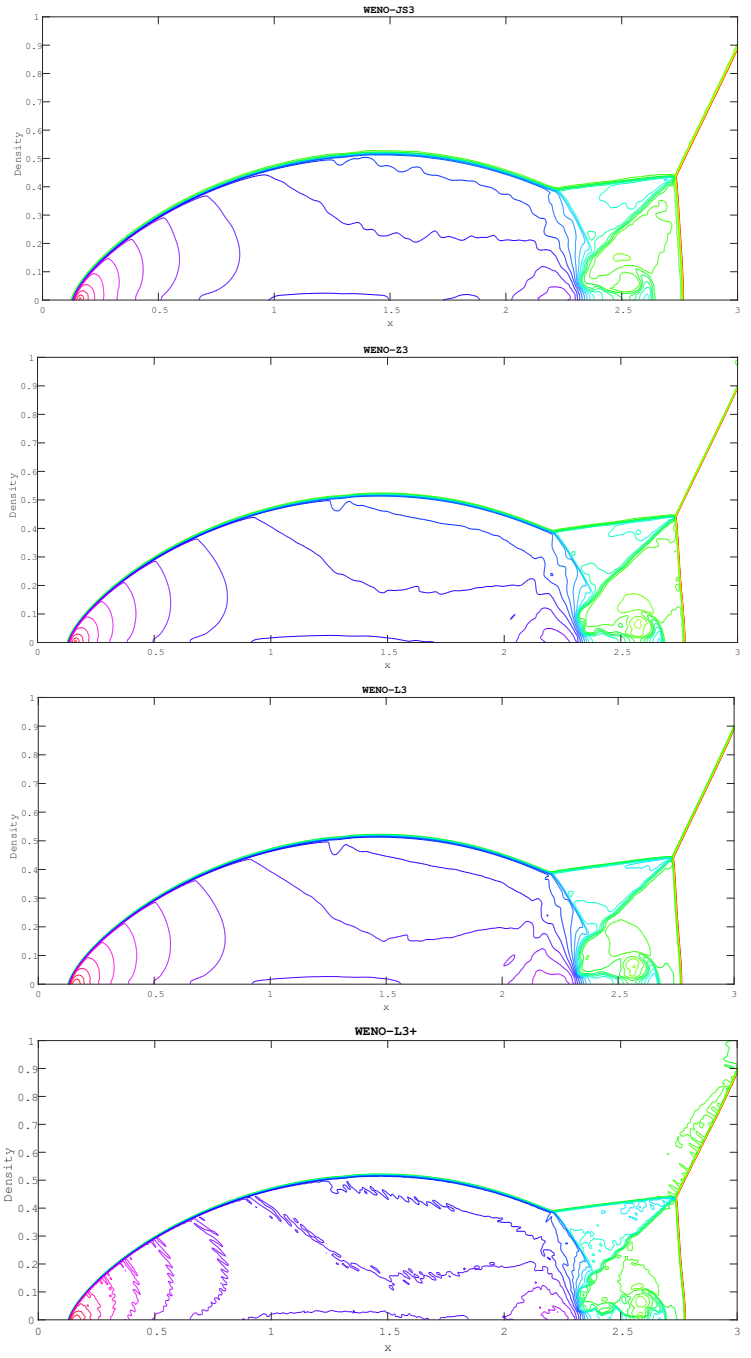

Figure 5: Density plots for double Mach reflection problem for WENO-JS3, WENO-Z3, WENO-L3 and WENO-L3+ schemes at time up to $t = 0.2$ with the grid points of 1920×480.

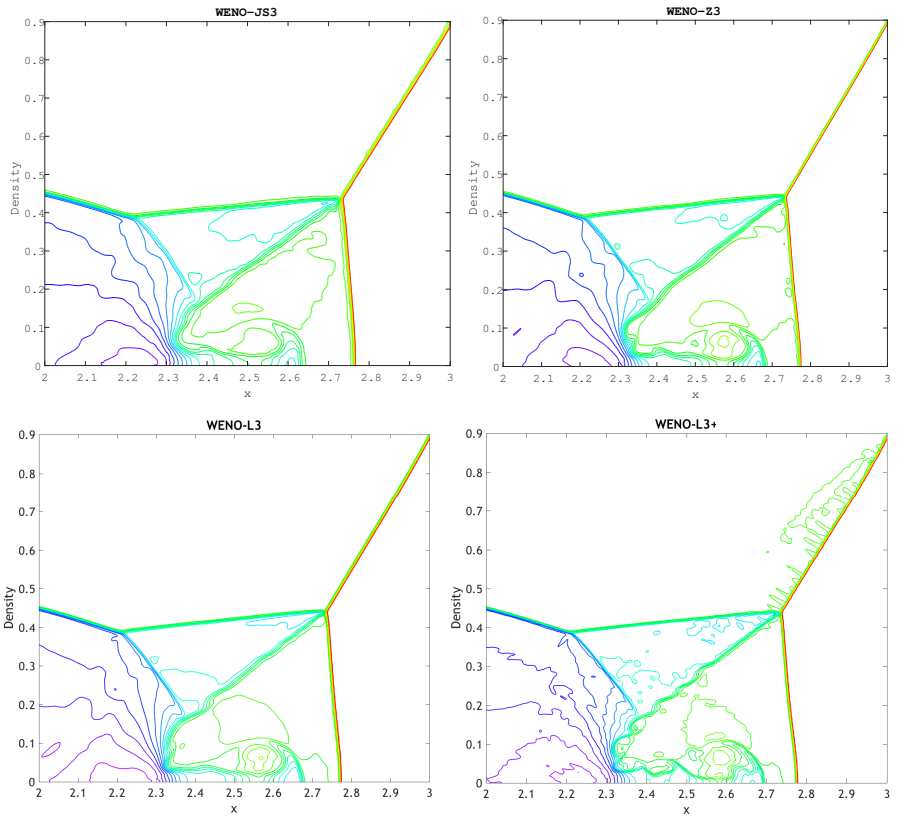

Figure 6: Close-up regions of density plots near double Mach stems for WENO-JS3, WENO-Z3, WENO-L3 and WENO-L3+ schemes at time up to $t = 0.2$ with the grid points of 1920×480.

[15] Y. Ha, C. H. Kim, Y. J. Lee, J. Yoon, *An improved weighted essentially non-oscillatory scheme with a new smoothness indicator*, Journal of Computational Physics **232** (1) (2013) 68–86.

[16] P. Fan, Y. Shen, B. Tian, C. Yang, *A new smoothness indicator for improving the weighted essentially non-oscillatory scheme*, Journal of Computational Physics **269** (2014) 329–354.

[17] F. Acker, R. d. R. Borges, B. Costa, *An improved WENO-Z scheme*, Journal of Computational Physics **313** (2016) 726–753.

[18] D. S. Balsara, S. Garain, C.-W. Shu, *An efficient class of WENO schemes with adaptive order*, Journal of Computational Physics **326** (2016) 780–804.

[19] W. Xu, W. Wu, *Improvement of third-order WENO-Z scheme at critical points*, Computers & Mathematics with Applications **75** (9) (2018) 3431–3452.

[20] W. Xu, W. Wu, *An improved third-order weighted essentially non-oscillatory scheme achieving optimal order near critical points*, Computers & Fluids **162** (2018) 113–125.

[21] A. Kumar, B. Kaur, *An Improvement of Third Order WENO Scheme for Convergence Rate at Critical Points with New Non-linear Weights*, Differential Equations and Dynamical Systems (2019) 1–19.

[22] A. Kumar, B. Kaur, R. Kumar, *A new fifth order finite difference WENO scheme to improve convergence rate at critical points*, Wave Motion **109** (2022) 102859.

[23] J. Zhu, J. Qiu, *A new fifth order finite difference WENO scheme for solving hyperbolic conservation laws*, Journal of Computational Physics **318** (2016) 110–121.

[24] J. Zhu, J. Qiu, *A new type of finite volume WENO schemes for hyperbolic conservation laws*, Journal of Scientific Computing **73** (2-3) (2017) 1338–1359.

[25] G. Li, X. Li, P. Li, D. Cai, *An improved third-order finite difference weighted essentially nonoscillatory scheme for hyperbolic conservation laws*, International Journal for Numerical Methods in Fluids **92** (12) (2020) 1753–1777.

[26] M. Sharma, A. Bhargava, S. Kumar, L. Rathour, L. N. Mishra, S. Pandey, et al., *A FERMATEAN FUZZY RANKING FUNCTION IN OPTIMIZATION OF INTUITIONISTIC FUZZY TRANSPORTATION PROBLEMS.*, Advanced Mathematical Models & Applications **7** (2) (2022).

[27] M. Sharma, N. Dhiman, S. Kumar, L. Rathour, V. N. Mishra, *Neutrosophic Monte Carlo simulation approach for decision making in medical diagnostic process under uncertain environment*, Int J Neutrosophic Sci **22** (1) (2023) 08–16.

[28] M. SHARMA, S. CHAUDHARY, L. RATHOUR, V. N. MISHRA, *Modified genetic algorithm with novel crossover and mutation operator for travelling salesman problem*, Sigma Journal of Engineering and Natural Sciences **42** (6) (2024).

[29] N. T. Negero, G. F. Duressa, L. Rathour, V. N. Mishra, *A novel fitted numerical scheme for singularly perturbed delay parabolic problems with two small parameters*, Partial Differential Equations in Applied Mathematics **8** (2023) 100546.

[30] M. S. Hogeme, M. M. Woldaregay, L. Rathour, V. N. Mishra, *A stable numerical method for singularly perturbed Fredholm integro differential equation using exponentially fitted difference method*, Journal of Computational and Applied Mathematics **441** (2024) 115709.

[31] G. Farid, S. Mehmood, L. Rathour, L. Mishra, V. Mishra, *Fractional Hadamard and Fejer-Hadamard inequalities associated with exp.(α, H- M)-convexity*, Dyn. Contin. Discr. Impuls. Syst. Ser. A: Math. Anal **30** (2023) 353–367.

[32] V. N. Mishra, L. N. Mishra, *Trigonometric approximation of signals (functions) in Lp)-norm*, International Journal of Contemporary Mathematical Sciences **7** (19) (2012) 909–918.

[33] F. Aràndiga, M. C. Martí, P. Mulet, *Weights design for maximal order WENO schemes*, Journal of Scientific Computing **60** (2014) 641–659.

[34] F. Aràndiga, A. Baeza, A. Belda, P. Mulet, *Analysis of WENO schemes for full and global accuracy*, SIAM Journal on Numerical Analysis **49** (2) (2011) 893–915.

[35] A. K. Henrick, T. D. Aslam, J. M. Powers, *Mapped weighted essentially non-oscillatory schemes: achieving optimal order near critical points*, Journal of Computational Physics **207** (2) (2005) 542–567.

[36] N. R. Gande, A. A. Bhise, *Modified third and fifth order WENO schemes for inviscid compressible flows*, Numerical Algorithms (2020) 1–31.

[37] C.-W. Shu, S. Osher, *Efficient implementation of essentially non-oscillatory shock-capturing schemes, II*, in: Upwind and High-Resolution Schemes, Springer, 1989, pp. 328–374.

[38] P. D. Lax, *Weak solutions of nonlinear hyperbolic equations and their numerical computation*, Communications on pure and applied mathematics **7** (1) (1954) 159–193.

[39] P. Woodward, P. Colella, *The numerical simulation of two-dimensional fluid flow with strong shocks*, Journal of computational physics **54** (1) (1984) 115–173.

[40] P. D. Lax, X.-D. Liu, *Solution of two-dimensional Riemann problems of gas dynamics by positive schemes*, SIAM Journal on Scientific Computing **19** (2) (1998) 319–340.

Author information

Anurag Kumar, Department of Mathematics, University of Delhi, Delhi-110007, India.
Department of Mathematics, School of Basic Sciences, Galgotias University, Plot No. 2, Sector 17 A, Yamuna Expressway, Greater Noida, Uttar Pradesh-203201, India.
E-mail: anuragkatiyar007@gmail.com

Bhavneet Kaur, Department of Mathematics, Lady Shri Ram College for Women, University of Delhi, Delhi-110024, India.
E-mail: bhavneet.lsr@gmail.com

Neeraj Kumar Tripathi, 58/46, Krishna Nagar, Allahabad Degree College, University of Allahabad, Kydganj, Prayagraj, Uttar Pradesh-211003, India.
E-mail: neerajktripathi13@gmail.com

Received: 2024-01-06
Accepted: 2024-06-15